20 March 1998

ELSEVIER

Chemical Physics Letters 285 (1998) 170–173

CHEMICAL PHYSICS LETTERS

Hydrogen bond strengths revealed by topological analyses of experimentally observed electron densities

E. Espinosa [a,b], E. Molins [a], C. Lecomte [b]

[a] *Institut de Ciència de Materials de Barcelona (CSIC), Campus de la UAB, 08193 Cerdanyola (Barcelona), Spain*

[b] *Laboratoire de Cristallographie et Modélisation des Matériaux Minéreaux et Biologiques, URA CNRS 809, Université Henri Poincaré, Nancy 1, BP 239, 54506 Vandoeuvre-lès-Nancy Cédex, France*

Received 25 November 1997; in final form 9 January 1998

Abstract

Interatomic interactions such as hydrogen bonds (HB) can be adequately described and classified by the topological properties of the electron density $\rho(\boldsymbol{r})$ at the $(3,-1)$ critical points $\boldsymbol{r}_{\mathrm{CP}}$ where the gradients of $\rho(\boldsymbol{r})$ vanish. We have analysed the topological properties of $\rho(\boldsymbol{r})$ at the intermolecular critical points of 83 experimentally observed HBs [X–H $\cdots$ O (X = C,N,O)], using accurate X-ray diffraction experiments. In spite of different models, methods and experimental conditions employed to obtain the topological properties of $\rho(\boldsymbol{r})$, we show that, for closed-shell interactions, the kinetic energy density $G(\boldsymbol{r}_{\mathrm{CP}})$ and the potential energy density $V(\boldsymbol{r}_{\mathrm{CP}})$ at the critical point depend exponentially on the H $\cdots$ O distance. Moreover, theoretical calculations for several HB dissociation energies follow the same law as does $V(\boldsymbol{r}_{\mathrm{CP}})$, with a simple change of scale. © 1998 Elsevier Science B.V.

In the framework of quantum theory, Bader's analysis allows us to study interatomic interactions in terms of the topological properties of the electron density $\rho(\boldsymbol{r})$ [1]. In this spirit, Abramov has recently proposed the evaluation of the local electronic kinetic energy density $G(\boldsymbol{r})$ from the experimental electron density distribution $\rho(\boldsymbol{r})$ [26]. Good agreement with Hartree–Fock calculations of $G(\boldsymbol{r})$ is obtained in the medium-range region, i.e. for distances ~ 0.5–2.1 Å from the atomic nuclei. In the H $\cdots$ O HB interaction, the valence shells of both atoms create a $(3,-1)$ bond critical point $\boldsymbol{r}_{\mathrm{CP}}$, which is observed experimentally from 0.5 to 1.2 Å from the hydrogen and from 1.0 to 1.6 Å from the oxygen nuclei, respectively. Therefore, the Abramov expression for closed-shell interactions at $\boldsymbol{r}_{\mathrm{CP}}$,

$$G(\boldsymbol{r}_{\mathrm{CP}}) = \tfrac{3}{10}(3\pi^2)^{2/3}\rho^{5/3}(\boldsymbol{r}_{\mathrm{CP}}) + \tfrac{1}{6}\nabla^2\rho(\boldsymbol{r}_{\mathrm{CP}}), \quad (1)$$

should be a good estimate of the local kinetic energy when HBs are concerned.

In order to analyse the $G(\boldsymbol{r}_{\mathrm{CP}})$ dependence on HB geometry, we have assembled topological and structural data from accurate electron density studies involving X–H $\cdots$ O (X = C,N,O) hydrogen bonds [2–15]. The *xyz* H coordinates taken from the above references are either derived from neutron data or

PII S0009-2614(98)00036-0

from X-ray: in the latter case, the X · · · H distance was constrained to the average neutron distance. The H · · · O distances range from 1.56 to 1.97 Å, from 1.65 to 2.63 Å and from 2.28 to 2.59 Å for O–H · · · O, N–H · · · O and C–H · · · O interactions, respectively. In Fig. 1, $G(\boldsymbol{r}_{CP})$ values obtained from Eq. (1) are represented versus their corresponding H · · · O distance. The estimated error for $G(\boldsymbol{r}_{CP})$ ranges from 5 to 15 kJ/mol (from the weaker to stronger observed HBs) and the maximum error on the H · · · O distance is 0.02 Å. The data were fitted by a simple unweighted exponential function $G(\boldsymbol{r}_{CP}) = a\exp(-bd)$, where d is the H · · · O distance and a and b are fitting parameters. The spread of the 83 points about the fitted line is narrow in spite of the different multipolar models (MOLLY [16], VALRAY [17], LSMOL [18] and POP [19]), methods (X–X, X–(X + N) and X–N)[9,20] and experimental conditions (temperatures, diffractometers, programs and laboratories) used in their determination. Also noticeable is the fact that C–H · · · O contacts (here observed with $d(\mathrm{H}\cdots\mathrm{O}) \geqslant 2.219$ Å), sometimes controversial in their consideration as HBs, seem to

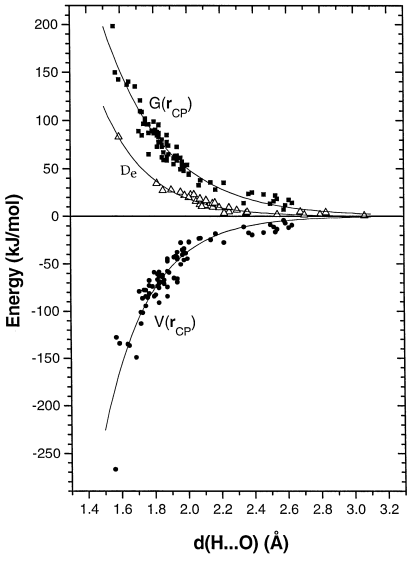

Fig. 1. Kinetic energy density $G(\boldsymbol{r}_{CP})$ (kJ/mol per atomic unit volume), potential energy density $V(\boldsymbol{r}_{CP})$ (kJ/mol per atomic unit volume) and dissociation energy D_e (kJ/mol) dependences on d(H · · · O) distance (Å). Solid lines correspond to the exponential fittings: $G(\boldsymbol{r}_{CP}) = 12(2)\times10^3\ \exp[-2.73(9)\ d(\mathrm{H}\cdots\mathrm{O})]$, $V(\boldsymbol{r}_{CP}) = -50.0(1.1)\times10^3\ \exp[-3.6\ d(\mathrm{H}\cdots\mathrm{O})]$ and $D_e = 25.3(6)\times10^3\ \exp[-3.6\ d(\mathrm{H}\cdots\mathrm{O})]$.

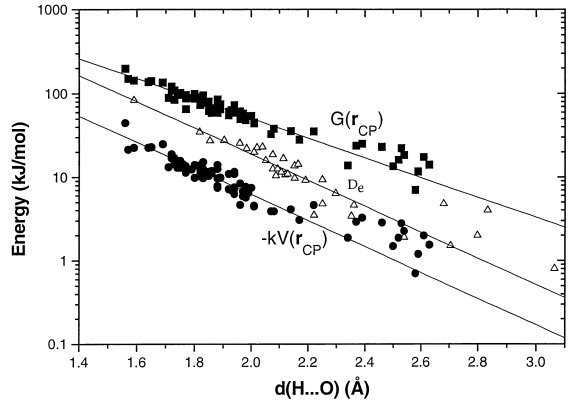

Fig. 2. Log–linear plot of $G(\boldsymbol{r}_{CP})$, $-kV(\boldsymbol{r}_{CP})$ and D_e versus d(H · · · O). The coefficient k has been selected equal to 1/6 in order to separate the depicted points.

follow the same phenomenological behaviour as the two other types N–H · · · O and O–H · · · O within errors. However, the systematic trend observed in Fig. 2 for distances greater than ≈ 2.3 Å reveal a low overlap between H and O clouds and therefore an almost pure electrostatic interaction. Further work in this direction is underway. The log–linear plot of $G(\boldsymbol{r}_{CP})$ against d(H · · · O) is linear (Fig. 2), indicating the exponential nature of the dependence. The corresponding exponential curve is shown in Fig. 1 as a solid line. The decrease of $G(\boldsymbol{r}_{CP})$ with increasing H · · · O hydrogen bond distance is a consequence of the similar behaviours found between both, $\rho(\boldsymbol{r}_{CP})$ and $\nabla^2\rho(\boldsymbol{r}_{CP})$, and d(H · · · O), as we have observed in an analysis of the 83 HBs. In this way, a decrease in the kinetic energy at $\boldsymbol{r}_{CP}$ is related to a lower electron density at that point because a lower accumulation of electrons implies less repulsion between them (see later the interpretation of $V(\boldsymbol{r}_{CP})$ and $G(\boldsymbol{r}_{CP})$). Theoretical calculations of $G(\boldsymbol{r}_{CP})$ in the HB region of the dimer $(H_2O)_2$ made by Bader and Essen [23] and by Abramov [26] give values of 42.0 and 39.4 (2.6) kJ/mol per atomic unit volume, respectively, for a distance $d(\mathrm{H}\cdots\mathrm{O}) = 2.039$ Å. Introducing that distance in our empirical equation relating $G(\boldsymbol{r}_{CP})$ to d(H · · · O) (see Fig. 1, caption), we obtain for $G(\boldsymbol{r}_{CP})$ a value of 45.9 kJ/mol per atomic unit volume, which is in good agreement with these theoretical calculations.

The local form of the virial theorem relates the Laplacian function of the electron density $\nabla^2\rho(\boldsymbol{r})$ to

both the local electronic kinetic energy density $G(\boldsymbol{r})$ and the local electronic potential energy density $V(\boldsymbol{r})$ [1]. Thus, at the H···O critical point, the potential contribution can be calculated using the $\nabla^2\rho(\boldsymbol{r}_{CP})$ and $G(\boldsymbol{r}_{CP})$ values,

$$V(\boldsymbol{r}_{CP}) = \frac{\hbar^2}{4m}\nabla^2\rho(\boldsymbol{r}_{CP}) - 2G(\boldsymbol{r}_{CP}). \quad (2)$$

The derived $V(\boldsymbol{r}_{CP})$ values for the 83 HBs are also represented as a function of the H···O distance in Fig. 1. Similarly to the $G(\boldsymbol{r}_{CP})$ dependence, $V(\boldsymbol{r}_{CP})$ follows an exponential dependence on H···O distance, although with a slightly different exponential factor, as shown in the log–linear plot of $V(\boldsymbol{r}_{CP})$ against d(H···O) (Fig. 2). The corresponding exponential curve is also shown in Fig. 1 as a solid line. As in the $G(\boldsymbol{r}_{CP})$ case, the decreasing of the $V(\boldsymbol{r}_{CP})$ magnitude with the increasing of d(H···O) is a consequence of the behaviours found between both, $\rho(\boldsymbol{r}_{CP})$ and $\nabla^2\rho(\boldsymbol{r}_{CP})$, and d(H···O). In this way, a lower electron density at $\boldsymbol{r}_{CP}$ is related to a decrease in the potential energy magnitude at that point because a weaker capacity to accumulate electrons at $\boldsymbol{r}_{CP}$ implies small $\rho(\boldsymbol{r}_{CP})$ values. Thus, we point out the positive correlation between all three magnitudes $\rho(\boldsymbol{r}_{CP})$, $G(\boldsymbol{r}_{CP})$ and $|V(\boldsymbol{r}_{CP})|$.

The relationship between the local electronic energy densities, $G(\boldsymbol{r}_{CP})$ and $V(\boldsymbol{r}_{CP})$, is shown in Fig. 3. Even though a proportional relationship can be assumed for weak HBs, an exponential fitting applies well for the whole range of H···O distances. Both magnitudes $V(\boldsymbol{r}_{CP})$, which represents the capacity of the system to concentrate electrons at the critical point and $G(\boldsymbol{r}_{CP})$, which gives the tendency of the system to dilute electrons at the same point, increase together as a consequence of the Pauli principle. In this way, and due to their observed correlation, $V(\boldsymbol{r}_{CP})$ can be interpreted as the action of the HB system to the electronic charge around the critical point and $G(\boldsymbol{r}_{CP})$ the corresponding reaction. Thus, $V(\boldsymbol{r}_{CP})$ and $G(\boldsymbol{r}_{CP})$ reflect, from two different points of view, a unique physical process, i.e. how the electrons around the critical point are affected by the HB interaction. As Bader pointed out [1], an energy density is dimensionally equivalent to a force per unit area, i.e. a pressure. Thus, we can interpret $V(\boldsymbol{r}_{CP})$ as the pressure exerted by the HB system on the electrons around the critical point, whereas $G(\boldsymbol{r}_{CP})$ is the pressure exerted (as a reaction) by those electrons on the HB system.

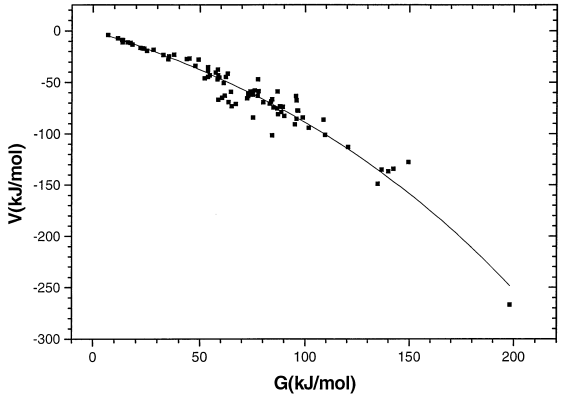

Fig. 3. $V(\boldsymbol{r}_{CP})$ versus $G(\boldsymbol{r}_{CP})$. The solid line represent the exponential fitting: $V(\boldsymbol{r}_{CP}) = 106(13)\,(1-\exp[6.1(5)\times10^{-3}\ G(\boldsymbol{r}_{CP})])$.

The boundary between shared and closed-shell interactions (i.e. $\nabla^2\rho(\boldsymbol{r}_{CP}) = 0$ or $V(\boldsymbol{r}_{CP}) = -2G(\boldsymbol{r}_{CP})$)[1] can be obtained by extrapolating the curve relating $V(\boldsymbol{r}_{CP})$ and $G(\boldsymbol{r}_{CP})$ in Fig. 3. This corresponds to $G(\boldsymbol{r}_{CP}) \approx 320$ kJ/mol per atomic unit volume, which in turn corresponds (see Fig. 1) to a H···O distance of ≈ 1.33 Å. Shorter HB distances should therefore be considered shared-shell interactions, which only appear in strong HBs [4,13]. The lower limit of 1.33 Å is thus an approximate threshold of validity for Eq. (1) and, therefore, for all the derived results of this work.

A relation between local energy densities at the critical point and the HB dissociation energy D_e is not straightforward. However, we have represented some HB dissociation energies as a function of d(H···O) on Fig. 1 together with $V(\boldsymbol{r}_{CP})$ and $G(\boldsymbol{r}_{CP})$. These values have been theoretically calculated from different ab initio SCF methods (restricted Hartree–Fock 6-311++G**//6-31G** calculations [21], Hartree–Fock calculations using the 6-31G** basis set [22,23], Hartree–Fock calculations using the 3-21+G** basis set at the crystal geometry [24] and both Hartree–Fock and second-order Møller–Plesset calculations using the D95++(d,p) and the 6-31 G(d,p) basis sets [25]). Fig. 2 shows that the distribution of the D_e data behaves as an exponential law against the H···O distance. The exponential factor of the fitting curve D_e (kJ/mol) $= 23(5)\times10^3\ \exp(-3.54(10)\ d(\mathrm{H}\cdots\mathrm{O}))$ is statis-

tically equivalent to the corresponding factor in the potential energy density fitting curve $V(\boldsymbol{r}_{CP})$ (kJ/mol per atomic unit volume) $= -54(18) \times 10^3$ exp($-3.65(18)$ d(H $\cdots$ O)). Fixing both exponential factors at -3.6 and fitting only the multiplier factors, we obtain $D_e = 25.3(6) \times 10^3$ exp(-3.6 d(H $\cdots$ O)) and $V(\boldsymbol{r}_{CP}) = -50.0(1.1) \times 10^3$ exp(-3.6 d(H $\cdots$ O)). This small variation in the parameters permits one to define equivalent exponential functions, which fit the same features without any statistically significant change. Therefore, a proportionality can be proposed between the HB energy ($E_{HB} = -D_e$) and $V(\boldsymbol{r}_{CP})$:

$$E_{HB} = \tfrac{1}{2} V(\boldsymbol{r}_{CP}), \qquad (3)$$

the proportionality factor being in volume atomic units. This equation points to a positive correlation between both energetic properties.

In conclusion, the H $\cdots$ O distance summarises the essential features of the HB interaction and, through its implicit relationship with the topological properties of the electron density at the critical point, it permits the correlation of the hydrogen bond energy (E_{HB}) to the pressure exerted on the electrons around the critical point ($V(\boldsymbol{r}_{CP})$), both related to the strength of the HB interaction.

Acknowledgements

E.E. and C.L. are grateful to Dr. G. T. DeTitta for helpful discussions. They are also grateful to Professor R.F.W. Bader for numerous discussions during his stay in the University of Nancy as an invited professor.

References

[1] R.F.W. Bader, Atoms in Molecules: a Quantum Theory (Clarendon Press, Oxford, 1990).
[2] M. Souhassou, C. Lecomte, R.H. Blessing, A. Aubry, M.M. Rohmer, R. Wiest, M. Bénard, M. Marraud, Acta Cryst. B47 (1991) 253–266.
[3] M. Souhassou, C. Lecomte, N. Ghermani, M.M. Rohmer, R. Wiest, M. Bénard, R.H. Blessing, J. Am. Chem. Soc. 114 (1992) 2371–2383.
[4] N. Pérès, Ph.D. Thesis, University of Henri Poincaré–Nancy 1, France, 1997.
[5] H. Lachekar, Ph.D. Thesis, University of Henri Poincaré–Nancy 1, France, 1997.
[6] R. Destro, F. Merati, Z. Naturforsch. 48a (1993) 99–104.
[7] R. Wiest, V. Pichon-Pesme, M. Bénard, C. Lecomte, J. Phys. Chem. 98 (1994) 1351–1362.
[8] R. Destro, R. Bianchi, C. Gatti, F. Merati, Chem. Phys. Lett. 186 (1991) 47–52.
[9] E. Espinosa, C. Lecomte, E. Molins, S. Veintemillas, A. Cousson, W. Paunslus, Acta Cryst. B52 (1996) 519–534.
[10] R. Bianchi, C. Gatti, V. Adovasio, M. Nardelli, Acta Cryst. B52 (1996) 471–478.
[11] S.T. Howard, M.B. Hursthouse, C.W. Lehmann, E.A. Poyner, Acta Cryst. B51 (1995) 328–337.
[12] W.T. Klooster, S. Swaminathan, R. Nanni, B.M. Craven, Acta Cryst. B48 (1992) 217–227.
[13] C. Flensburg, S. Larsen, R.F. Stewart, J. Phys. Chem. 99 (1995) 10130–10141.
[14] V. Pichon-Pesme, C. Lecomte, Acta Cryst. B54 (1998) in press.
[15] R.F. Stewart, in: Eds. G.A. Jeffrey, J.F. Piniella, The Application of Charge Density Research to Chemistry and Drug Design, Vol. 250, (NATO ASI Series, Physics, Plenum Press, New York, 1991) pp. 63–101.
[16] N.K. Hansen, P. Coppens, Acta Cryst. A34 (1978) 909–921.
[17] R.F. Stewart, M.A. Spackman, VALRAY User's Manual (Department of Chemistry, Carnegie–Mellon University, Pittsburgh, PA, USA, 1983).
[18] T. Koritsanszky, LSMOL Program (SUNY Buffalo, NY, USA, 1987).
[19] B.M. Craven, H.P. Weber, X.M. He, The POP Least-Squares Refinement Procedure (Department of Crystallography, University of Pittsburgh, Pittsburgh, PA, USA, 1987).
[20] P. Coppens, Science 158 (1967) 1577–1579.
[21] M.T. Carroll, R.F.W. Bader, Mol. Phys. 65 (1988) 695–722.
[22] J.R. Cheesman, M.T. Carrol, R.F.W. Bader, Chem. Phys. Lett. 143 (1988) 450–458.
[23] R.F.W. Bader, H. Essen, J. Chem. Phys. 80 (1984) 1943–1960.
[24] K.J. Lin, M.C. Cheng, Y. Wang, J. Phys. Chem. 98 (1994) 11685–11693.
[25] L. Turi, J.J. Dannenberg, J. Phys. Chem. 97 (1993) 7899–7909.
[26] Yu.A. Abramov, Acta Cryst. A53 (1997) 264–272.